Vibrational Spectroscopy investigation of swelling phenomena in cyclodextrin nanosponges

ARTICLE *in* JOURNAL OF RAMAN SPECTROSCOPY · OCTOBER 2013

Impact Factor: 2.67 · DOI: 10.1002/jrs.4282

Research article

Journal of RAMAN SPECTROSCOPY

Received: 14 October 2012 Revised: 30 January 2013 Accepted: 30 January 2013 Published online in Wiley Online Library

(wileyonlinelibrary.com) DOI 10.1002/jrs.4282

Vibrational spectroscopy investigation of swelling phenomena in cyclodextrin nanosponges†

Franca Castiglione,[a] Vincenza Crupi,[b]* Domenico Majolino,[b] Andrea Mele,[a] Barbara Rossi,[c,d] Francesco Trotta[e] and Valentina Venuti[b]

The swelling behaviour of β-cyclodextrin nanosponges, a new class of polymers obtained by reacting β-cyclodextrin with pyromellitic dianhydride, has been here investigated by the analysis of the vibrational dynamics performed by using Fourier-transform infrared spectroscopy in Attenuated Total Reflectance geometry and Raman scattering. The measurements have been carried out at different hydration levels and in the temperature range 250 K–310 K. The decomposition and assignment of the spectral components of the O–H stretching band have been discussed in terms of water molecules engaged in different hydrogen bonding networks, allowing us to recognize three different 'types' of water, namely 'bonded', 'intermediate'and 'free'. By following this approach, a detailed picture of the connectivity pattern of water molecules inside the polymeric matrix is achieved. The analysis of HOH bending vibrational band gives further information perfectly consistent with the results obtained from the analysis of the O–H stretching spectral region. Copyright © 2013 John Wiley & Sons, Ltd.

Keywords: cyclodextrin nanosponges; FTIR-ATR spectroscopy; Raman spectroscopy; swelling; polymers; O–H stretching

Introduction

Cyclodextrins (CDs) are natural cyclic oligosaccharides with a characteristic central hydrophobic cavity and an hydrophilic outer surface, well known for their ability to form non-covalent inclusion complexes with a large variety of guest molecules[1,2]. Thanks to this capability, CDs have attracted considerable interest over the years opening the route to a large number of applications as vectors for the transport of active bio-molecules[3] in different technological fields, offering in particular numerous advantages in the case of pharmaceutical applications[4–6].

Nevertheless, CDs are, for example, unable to form inclusion complexes with hydrophilic substances or molecules of high molecular weight (i.e. proteins or enzymes) and they can easily dissociate from the guest molecule as a consequence of dilution[7]. In recent years, then, many efforts have been directed to develop new CD-based carrier systems with the aim to improve the performance of these oligosaccharides as host molecules.

Among the numerous CD-based derivatives designed to date, CD nanosponges (CDNS) have attracted a special interest for their remarkable capacities of inclusion and release of different types of molecules and macromolecules[8–11]. They are a new class of highly cross-linked polymers obtained by chemical reaction of CDs with suitable cross-linking agents, such as carbonyldiimidazole (CDI), pyromellitic dianhydride (PMA) or ethylenediaminetetraacetic acid dianhydride. The main feature of the nano-porous structure of CDNS is the simultaneous presence of both hydrophobic cavities of CD and hydrophilic nano-sized spaces existing among the individual units of the macrocycles. CDNS are generally insoluble in water and in common organic solvents, even if some classes of them exhibit intriguing properties of swelling in the presence of aqueous solutions, giving rise to a gel-like behaviour, similar to hydrogels. Due to these unique properties, CDNSs have been shown to be an extremely versatile material which has been exploited in a variety of fields, including agriculture[12], environmental control[13,14], manufacturing research[15,16] and pharmaceutical applications[17–25]. Nevertheless, despite the growing number of technological applications of nanosponges, many questions concerning the structure and the physicochemical properties of these polymers are still open. This is mainly due to the difficulty of investigating CDNS at the molecular level, because of the random nature of the growth process of the polymer.

In this context, the vibrational dynamics of two classes of nanosponges obtained by polymerization of β-CD with CDI (β-CDCDI) and PMA (β-CDPMA) has been recently investigated, in

* Correspondence to: Vincenza Crupi, Dipartimento di Fisica e di Scienze della Terra, Università di Messina, Viale Ferdinando Stagno D'Alcontres 31, 98166 Messina, Italy E-mail: vcrupi@unime.it

† This article is from the GISR part of the joint special issue on the European Conference on Nonlinear Optical Spectroscopy (ECONOS 2012) with Guest Editors Johannes Kiefer and Peter Radi and the II Congresso Nationale di Spettroscopie Raman ed Effetti Ottici Non Lineari (GISR 2012) with Guest Editor Maria Grazia Giorgini.

a Dipartimento di Chimica, Materiali e Ing. Chimica 'G. Natta', Politecnico di Milano, via L. Mancinelli 7, 20131 Milano Italy

b Dipartimento di Fisica e di Scienze della Terra, Università di Messina, Viale Ferdinando Stagno D'Alcontres 31, 98166 Messina Italy

c Dipartimento di Informatica, Università di Verona, Strada le Grazie 15, 37134 Verona Italy

d Dipartimento di Fisica, Università di Trento, via Sommarive 14, 38123 Povo Trento, Italy

e Dipartimento di Chimica, Università di Torino, Via P. Giuria 9, 10125 Torino Italy

the dry state, by the combined use of Raman and Fourier-transform infrared spectroscopy in Attenuated Total Reflectance (FTIR-ATR) spectroscopy, in different wavenumber regimes[11,26–29]. These studies provided a detailed characterization of these polymers at molecular level, giving indication that the cross-linking degree and the stiffness of the material can be effectively modulated by properly choosing the type of cross-linking agent and by varying the molar ratio between CD and cross-linker during the reaction of polymerization. In particular, a maximum in the cross-linking and stiffness of the polymeric network of PMA-nanosponges has been found for a sixfold excess of PMA with respect to β-CD[27,29].

In addition, high-resolution magic angle spinning nuclear resonance spectroscopy was used to investigate swollen β-CDPMA nanosponges[28]. The results of this study suggest the existence of two different states of water molecules inside the gel phase, i.e. 'free' and 'bound' water.

In this work, by using FTIR-ATR and Raman spectroscopy, we explore the vibrational dynamics of water molecules into the swollen β-CDPMA nanosponges, as a function of (1) cross-linking degree of the polymer, (2) level of hydration and (3) temperature, with the aim to investigate the water–polymer interactions and the hydrogen bonds (HBs) network of water molecules in the gel phase.

This study is a preliminary and crucial step to more deeply understand the molecular basis of the swelling phenomena in CDNS, which is in turn strongly related to the inclusion and release properties inside the polymeric matrix of this innovative soft material.

Experimental methods

Synthesis of nanosponges and preparation of gels

The CDNSs β-CDPMA14, β-CDPMA16 and β-CDPMA110 were obtained by following the synthetic procedure already described in previous works[27,29].

The reactions of polymerization between β-CD and the cross-linking agent PMA, at β-CD:PMA molar ratios of 1:*n* (with $n = 4, 6, 10$) were conducted dissolving the reagents in dimethyl sulfoxide (DMSO) containing triethylamine and allowing them to react at room temperature for 3 h. Once the reaction was over, the solid obtained was ground in a mortar and Soxhlet extracted with acetone for 8 h.

The gels of CDNSs were prepared by adding to the powder samples of β-CDPMA1*n* ($n = 4, 6, 10$) a suitable amount of double-distilled and deionized water (Sigma) in order to obtain two different levels of hydration h = 3.3 and 5, where h is defined as weight ratio H_2O/β-CDPMA1*n*.

All the samples of gel were freshly prepared and used for both FTIR-ATR and Raman measurements.

FTIR-ATR measurements

FTIR-ATR studies were carried out on a DA8 FTIR spectrometer from BOMEM, using a thermo-electrically cooled deuterated triglycene sulphate detector, in combination with a KBr beamsplitter and a Globar source. For all the investigated samples, measurements were performed in the T-range 250 K–310 K. The gels were contained in a Golden Gate diamond ATR system, based on the ATR technique[30]. The spectra were recorded in the O–H stretching and HOH bending mode wavenumber regions, 2800–3800 cm^{-1} and 1500–1800 cm^{-1}, respectively. Each spectrum was collected with a resolution of 4 cm^{-1} and is an average of 100 repetitive scans, so guaranteeing a good signal-to-noise ratio and high reproducibility. No smoothing was done, and spectroscopic manipulation such as baseline adjustment and normalization were performed using the Spectracalc software package GRAMS (Galactic Industries, Salem, NH, USA). Band decomposition was undertaken using the curve fitting routine provided in the PeakFit 4.0 software package, which enabled the type of fitting function to be selected. The strategy adopted was to use well-defined shape components of Voigt functions with all the parameters allowed to vary upon iteration. The statistical parameters were used as a guide to 'best fit'.

Raman scattering measurements

Raman spectra were recorded on the samples of gels inserted into an optical quartz cell, at room temperature and in crossed polarization. All the spectra were collected in the wavenumber range 100–3700 cm^{-1}. The exciting radiation at 632.8 nm (He–Ne laser, power at the output ≈ 20 mW) was focused onto the sample surface through the 10X objective of a microprobe setup (Horiba-Jobin-Yvon, LabRam Aramis) consisting of a 46 cm focal length spectrograph using a 1800 grooves/mm grating and a charge-coupled device detector. The elastically scattered radiation was filtered by using a narrow-band edge filter. The resolution was about 0.35 cm^{-1}/pixel.

Results and discussion

As well established[31], the presence, in H-bonded liquids, of the highly anisotropic and directional HB gives rise to several kinds of intra- and intermolecular arrangements.

Taking into account all the contributions composing the potential energy surface of the HB (electrostatic, polarization, charge transfer, dispersion), a strict correlation between the degree of association and the relative population of the local structures is expected, generating, in turn, a different dynamical response: this explains the appearance of peculiar bands according to the number of possible associative species[32]. On the basis of the cross-links among the inherent structures, corresponding to the various local minima in the potential energy, it is possible to explain the spectral variation, for H-bonded liquids, of the O–H stretching vibration, which spreads out over a large ω-range and changes dramatically in frequency (red shift), shape and intensity with respect to the original narrow O–H band centred at ~ 3630 cm^{-1}. Although these changes are an almost clear evidence of intra- and intermolecular O···H bonding effects, they are difficult to explain by a unique theoretical model. For example, the factors should be taken into account to explain the band shift effects and the potential surface shapes can be derived by quantum mechanical computation and/or anharmonic coupling of the O–H fundamental vibration with low-frequency intermolecular modes due to intermolecular interactions.

Water is a three-dimensional interconnected network of HBs, which, from experimental and theoretical results, is believed to determine its special physical structure. This is because, considering that the HB lifetime lies in the subpicosecond timescale, the rearrangement continuously occurs and the spatial network results are well-defined for the most of time. Most of the structural models describing water either as a continuum

Journal of RAMAN SPECTROSCOPY

of geometries and energies or as a mixture of discrete species were not sufficient for an exhaustive explanation of its broad physical properties. Vibrational spectroscopy turned out to be a powerful tool for investigating structural correlations in water, and, if the electronic transitions involved in the Raman spectrum can induce some additional complexity[33], IR spectroscopy exhibits the relevant advantage of directly probing the interactions of the oscillators, coupling to the ground state of the molecules[34]. How the local structure relates to vibrational spectroscopy is still a controversial question. Generally, the complex structure of the O–H stretching mode is widely believed to be related to the structure of water[35,36], and although this mode is strictly probing vibrations along the O–H bond, the influence of neighboring HBs alter the intramolecular O–H bond and thus the dipole moment and vibrational spectra[37].

The decomposition of the O–H stretching band of water, by means of curve-fitting procedure, and the assignment of the vibrational components physical and molecular origin are necessary steps to obtain these structural information[30]. On these bases, it became customary to analyze O–H stretching spectra by considering several classes of O–H oscillators, at least two general classes involving H-bonded and non-H-bonded molecules. It's true that these classes, however, encompass broad components, each of which refers to structures that involve a range of bond angles and distances distributed around the component peak position[38]. Again, these structures have to be considered as *transient*, owing to the continuous breaking and reforming process of the H-bond, whose mean lifetime is, as we said, on the subpicosecond time scale. Assignments of each component and interpretation were reported in literature in different ways[39–41]. In general, the classification of O–H groups is based on the HB ordering parameters, O–H groups with a higher degree of HB order showing a band at a lower wavenumber[30].

Taking these considerations into account, Fig. 1 shows the FTIR-ATR (a) and Raman spectra (c) of the O–H stretching region (from ~ 2800 cm^{-1} to ~ 3800 cm^{-1}) of β-CDPMA1*n* nanosponges gels, as a function of the molar ratio *n*, for h = 5 and T = 290 K, as example. In the case of FTIR-ATR spectrum, the O–H stretching band appears superimposed to the C–H stretching profile, whose contribution, instead, is well resolved in the Raman spectrum.

Figure 1(a–c) points out a shift toward higher wavenumbers of the total O–H spectral profile when passing from $n = 4$ to $n = 6$. This finding suggests that increasing the cross-linking degree of the polymer brings about a destructuring effect on the intermolecular H-bonds network of water molecules. On the contrary, on passing from $n = 6$ to $n = 10$, the opposite wavenumber shift is observed. This trend is similar to what already found by previous FTIR-ATR and Raman results on the same systems in the dry state[27,29]. In that case, spectral data indicated that the maximum cross-linking level and stiffness of the polymeric network of PMA-nanosponges was reached for a sixfold excess of PMA with respect to β-CD. This was probably due to steric effects that tend to prevent further cross-linking of the polymer for higher molar ratios. It is then reasonable to think that the saturation of all the PMA reactive sites in the β-CDPMA110 nanosponge can prevent the water–polymer interactions favouring the water–water ones, and, hence, the possibility, for H_2O molecules, to develop, in the gel phase, highly-coordinated, long-range, H-bonded environments.

The same conclusions can be achieved by the analysis of the HOH bending region (from ~ 1500 cm^{-1} to ~ 1800 cm^{-1}) shown in Fig. 1(b–d). As already established, the intensity of the band assigned to intramolecular HOH bending mode of bulk liquid water diminishes with decreasing temperature and tends to zero at the crystallization[42]. This reduction upon cooling can be connected with the loss of induced transition dipole moment through the bending motion. In addition, a shift towards higher frequencies of the band maximum was observed as the temperature decreases. Based on these considerations, the HOH bending band has been ascribed to the water molecules not involved in a symmetric tetrahedral network[38,42]. Furthermore, the presence of a single absorption band also suggests that this mode is not affected by the intermolecular HB water network,

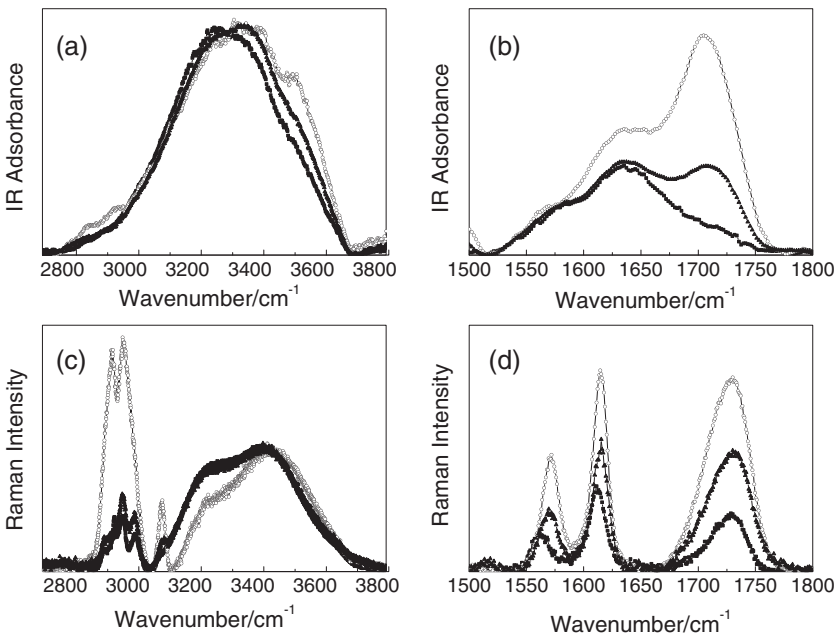

Figure 1. FTIR-ATR and Raman spectra in the O–H stretching region ((a) and (c), respectively) and in the HOH bending region ((b) and (d), respectively) of β-CDPMA1*n* nanosponges, as a function of molar ratio *n*, at h = 5 and T = 290 K. $n = 4$: closed squares, $n = 6$: open circles, $n = 10$: closed-up triangles.

in contrast to the composite O–H stretching band, whose substructures pertain to the differences in connectivity of the water molecules. As a consequence, the HOH bending spectral region is easier to analyse than the multiple band highly convoluted water stretching zone. Figure 1(b–d) displays the evolution, as a function of *n*, of the FTIR-ATR and Raman spectral profiles in the HOH bending region of β-CDPMA1*n* nanosponges gels at h = 5 and T = 290 K, as example. In the case of FTIR-ATR measurements, the HOH bending contribution appears as a relative intense and broad band centred at ~ 1640 cm^{-1}, convoluted with those ascribed to the PMA ring breathing modes (shoulder at ~ 1580 cm^{-1}) and to the C = O stretching of the cross-linker moiety (band ~ 1720 cm^{-1})[29]. Spectra of Fig. 1 (b–d) clearly indicate that the intensity of HOH bending mode is strong in the IR spectrum and very weak in the Raman one, thus strongly supporting the use of IR spectroscopy for the investigation of such vibrational mode. On the other side, Raman spectroscopy turns out to be ideal for the analysis of the evolution of the C = O stretching vibration. Indeed, the C = O stretching vibration mode is well separated from the other modes, observed at ~ 1570 cm^{-1} and 1615 cm^{-1}, corresponding to the PMA breathing ring vibrations.

It is interesting to observe the evolution of FTIR-ATR band associated to the HOH bending mode on passing from *n* = 4 to *n* = 6. This band swells over its low-wavenumber wing, with a corresponding shift of the band maximum towards lower energies. At the same time, the observed intensity increases. These results are consistent with those discussed above on the O–H stretching spectral region. They confirm that the increasing of the cross-linking degree of the polymer contributes to break the extended, tetrahedral arrangements of water molecules, thus favouring the organization of water molecules in not fully bonded networks. Once again, a progressive shift of bending centre-wavenumber towards the higher energies can be observed on passing from *n* = 6 to *n* = 10, together with a reduction of the band intensity. This finding suggests that an increasingly higher fraction of water molecules are arranged in high-coordination patterns.

The behaviour of the carbonyl stretching vibration in gel phase, whose intensity is proportional to the grade of cross-linking of the nanosponge network, reveals a maximum in the reticulation corresponding to sixfold excess of cross-linker with respect to β-CD, confirming also what already revealed in the case of dry PMA-nanosponges[29].

Figure 2(a–c) shows the FTIR-ATR and Raman spectrum in the O–H stretching region of β-CDPMA14 nanosponge, as a function of the hydration level h, at T = 290 K, as example. In the inset of each figure, the corresponding spectrum of bulk water at the same temperature is reported for comparison. At h = 3.3, a relevant shift of the band maximum towards the high-wavenumber region with respect to the bulk state is observed. This allows us to hypothesize that the confinement in the polymeric network induces the water molecules to assume arrangements with reduced cooperativity with respect to the bulk water, due to their interactions with surface active sites as well as of the topology of the interconnected pores. This is in agreement with what already observed in a variety of confined systems at low hydration levels[43,44]. By increasing the water content by passing from h =3.3 to h = 5, it is expected that a first layer of water molecules at the polymer interface tends to saturate the active sites of the polymer surface, thus causing an increase of water molecules arranged in a bulk-like structure with stronger HB. This is consistent with the experimental evidence of an increasing of the low-wavenumber contribution with the complementary decrease of the high-wavenumber one, together with a low-wavenumber shift of the maximum of the O–H stretching band. To further support this interpretation, the HOH bending region can be considered (Fig. 2(b–d)): indeed, the analysis of the vibrational spectra shows a shift towards higher wavenumbers of the HOH bending band and a intensity reduction.

The vibrational dynamics of water molecules is finally discussed as a function of temperature. In Fig. 3(a), we show the FTIR-ATR

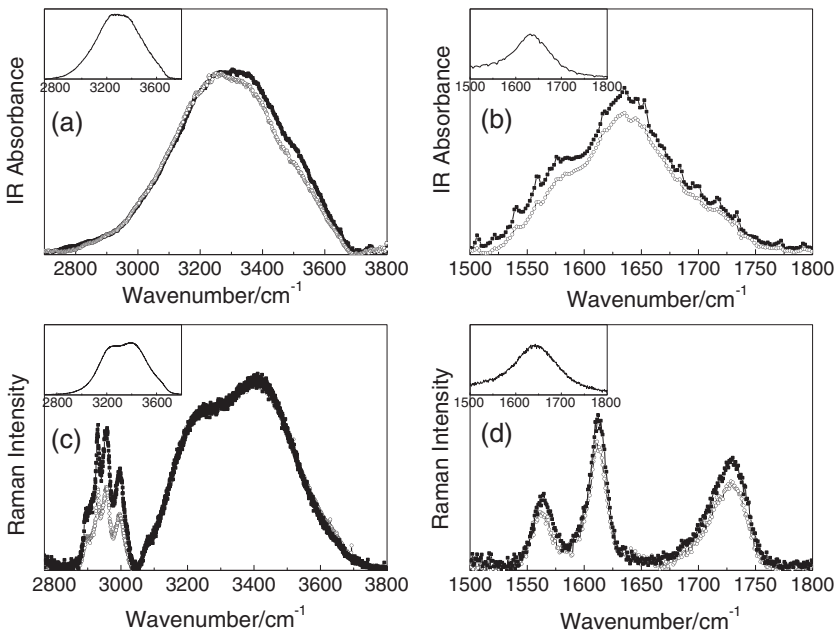

Figure 2. FTIR-ATR and Raman spectra in the O–H stretching region ((a) and (c), respectively) and HOH bending region ((b) and (d), respectively) of β-CDPMA14 nanosponge, as a function of the hydration level h, at T = 290 K. h = 3.3: closed squares, h = 5: open circles. In the inset of each figure, the corresponding spectrum of bulk water at the same temperature is reported for comparison.

Journal of RAMAN SPECTROSCOPY

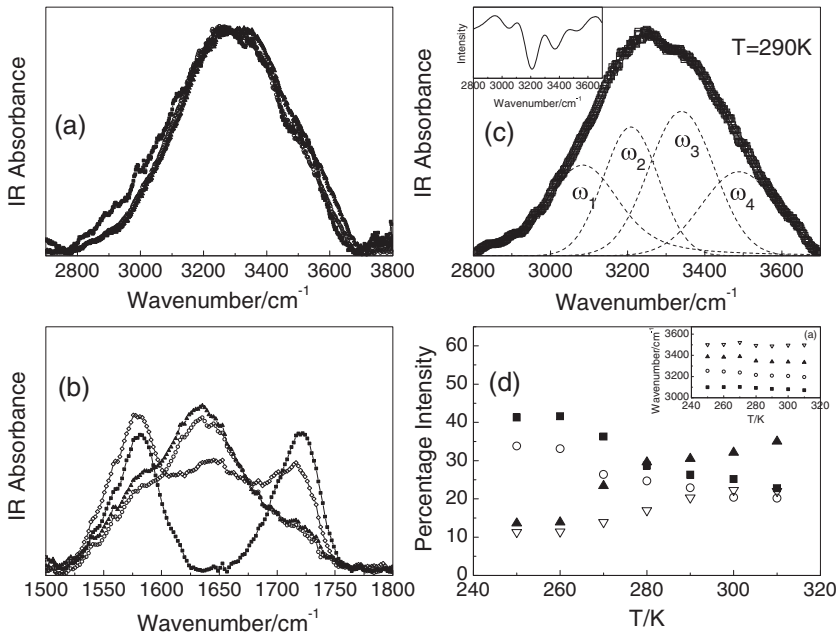

Figure 3. FTIR-ATR spectra in the O–H stretching (a) and HOH bending region (b) for β-CDPMA14 nanosponge, at h = 5, as a function of T. For the O–H stretching region: only T = 250 K (closed squares), 290 K (open circles), and 310 K (closed-up triangles) are reported for clarity. For the HOH bending region: only T = 250 K (closed squares), 270 K (open diamonds), 290 K (open circles), and 310 K (closed-up triangles) are reported for clarity. Again, panel (c) reports the FTIR-ATR spectrum in the O–H stretching region, together with the total best-fit (continuous line) and the decomposition components (dashed lines), for β-CDPMA14 at h = 5 and T = 290 K. Inset: calculated second derivative profile of the experimental spectrum for the same sample. Finally, panel (d) and its inset show, respectively, the T-dependence of percentage intensities I_i (i = 1, 2, 3, 4) and of the peak wavenumbers ω_i (i = 1, 2, 3, 4) of the different spectral contributions to the FTIR-ATR O–H stretching band for β-CDPMA14 nanosponge at h = 5. i = 1: closed squares, i = 2: open circles, i = 3: closed-up triangles, i = 4: open down triangles.

O–H stretching region for β-CDPMA14 nanosponge, at h = 5 and T = 250 K, 290 K, 310 K, as examples. The observed trend, as expected, recalls the well-known bulk-like water behaviour, i.e. with increasing T the O–H stretching band maximum shifts to higher wavenumber and the high-energy contribution becomes more and more relevant, giving evidence of a decreasing of H-bond strength and networking. The tendency of the thermal motion to destroy extended, tetrahedral arrangements in favour of the organization of water molecules in loosely tight networks is also evident from the HOH bending evolution as a function of T, as shown in Fig. 3(b). The band maximum shifts to lower energies, moving from ~ 1646 cm^{-1} to ~ 1634 cm^{-1}, and, at the same time, its intensity increases, starting from a just pronounced bump at T = 250 K and becoming the most relevant component in the spectrum at T = 310 K. It is worth of note that the intensity of this band remains relatively high even at T = 270 K, then it tends to disappear at T = 250 K. This is in contrast with what is observed in the case of bulk water.

A possible rational for this finding is that, in the explored temperature range, a certain population of confined water molecules in liquid-like state is still present, providing evidence of a supercooled behaviour already found for water entrapped in amorphous porous materials and phyllosilicates[45–47].

The investigation of the effect of temperature on the structural arrangements of confined water was accomplished through the decomposition of the FTIR-ATR O–H band into Voigt profiles. The presence in the experimental spectra of four sub-bands with the assigned centre frequencies was suggested by the analysis of the second derivative profiles that showed four minima approximately corresponding to the maxima of each band component[48]. (see, as example, the case of β-CDPMA14 at h = 5 and T = 290 K reported in the inset of Fig. 3(c)). Then, four components for the O–H stretching band have been used to describe the existing types of hydrogen-bonded OH oscillators. The obtained sub-bands are reported in Fig. 3(c) for β-CDPMA14 at h = 5 for T = 290 K, as example. The well-known difficulties[49,50] of uniquely fitting IR band profiles must lead to caution against overinterpretation of the data. Nevertheless, the procedure applied here, consisting of the evaluation of the minima in the second derivative profile of the measured spectra as a first indication of the peak wavenumbers of the corresponding components of the analysed band, allowed us in some way to overcome this difficulty. Furthermore, we remark that this is a well-established procedure employed in a lot of high-quality published papers when analyzing O–H stretching spectra of water in a variety of systems[29,48,51,52]. Finally, we underline that the protocol adopted here uses the minimum number of parameters and, at the same time, it furnishes extremely good fits to the data. The best-fit is, in fact, characterized by $r^{[2]}$ ~ 0.9999 for all the investigated systems.

For each sub-band, the peak wavenumbers ω_i (i = 1, 2, 3, 4) will account for the strength of the corresponding HBs. In our case, the largest observed wavenumber shift is less than 20 cm^{-1}, which, as a matter of fact, can be considered as constant (see the inset of Fig. 3(d)).

The respective fractions I_i/I_{tot} (i = 1, 2, 3, 4, expressed in % in Fig. 3(d)) of the different O–H band Voigt areas, describing the population of the corresponding OH oscillators, exhibit a different behaviour as a function of temperature.

The two sub-bands I_1 (closed squares) and I_2 (open circles) at the lowest wavenumbers decrease when T increases, whereas for the two high-wavenumber contributions I_3 (closed-up triangles) and I_4 (open down triangles), the opposite trend is revealed. Based on the well-known destructuring effect of the thermal motion, and considering the interpretation of the O–H stretching

vibration of confined water reported in the literature[53], we can assign the sub-bands ω_1 and ω_2 to the symmetric and asymmetric O–H stretching of tetrahedral structures having strong hydrogen bonding on both the hydrogen atoms, respectively. The sub-band ω_3 is assigned to the non-in-phase O–H stretching mode of tetrahedral arrangements commonly referred to as 'bifurcated H-bonds'[54], originating *distorted* tetrahedral structures. Finally, the band centred at ω_4 accounts for H_2O molecules for which HB has been partly or totally disrupted.

The non-null intensity of I_1 and I_2 in the examined temperature range indicates that confined water molecules can be involved in extended transient hydrogen-bonded networks with a high degree of connectivity, in spite of thermal motion, topological restrictions and surface interactions, thus confirming what observed (vide supra) by the analysis of the HOH bending mode. Their observed T-dependence is in a way expected, since far from crystallization more and more H_2O molecules will leave the tetrahedral arrangements.

The values of I_3 increase with temperature: this finding suggests that the high temperature tends to favour restricted connectivity structures, i.e. the bifurcated H-bonds between two water molecules. The opposite trend of I_1 and I_2, on one side, and I_3, on the other side, with increasing temperature allowed us to hypothesize a transfer process involving the relative population factors of tetrahedral networks with linear H-bonds and aggregates exhibiting distorted, bifurcated H-bonds.

Finally, the behaviour of I_4 shows an initial increase with temperature and a plateau in the high temperature range of the explored T interval. It is reasonable to assume that I_4 is related to the population of water molecules not taking part in the organization of higher connectivity structures. These water molecules are likely to saturate the hydrophobic void cavities of the CD polymer, thus accounting for the observed invariance of their population with temperature.

Conclusion

The swelling phenomenon of PMA-nanosponges is here investigated by an analysis of their vibrational dynamics through FTIR-ATR and Raman spectroscopies, in order to gain information on the water–polymer interactions and the structural properties of 'bound', 'intermediate' and 'free' water molecules inside the polymeric network, as a function of cross-linking degree of the polymeric matrix, hydration level and temperature.

According to what already revealed for the same systems in the dry state, a maximum cross-linking level and stiffness of the polymeric network of PMA-nanosponges was reached for a sixfold excess of PMA with respect to β-CD, probably due to steric effects that, in the gel phase, seem to promote, for further increasing of the cross-linker amount, the development of long-range, high-coordination, H-bonded environments for the entrapped water molecules. Surface active sites as well as the topology of the interconnected pores will both play a destructuring role in the HB network of confined water with respect to the bulk state, these modifications being more enhanced at low hydration level. Furthermore, thermal motion is, as expected, found to destroy extended, tetrahedral arrangements in favour of the organization of water molecules in loosely tight networks, and evidence of a supercooled behaviour of confined water is furnished. Finally, the analysis, using second-derivative computations and curve fitting, the O–H stretching vibration, as a function of temperature, provided information on the different degree of coordination of water molecules involved in various hydrogen bonding structures, highlighting at the same time the most energetically favoured environments.

The obtained information appear to be relevant for the prediction and control of the entrapping properties of 'guest' molecules by CDNS, from which shedding light on the complexation of drugs in host nanocarriers in solid phase and opening the way for the description of interactions in complexed supramolecular species host/drug and host/drug/receptor in the framework of the drug delivery.

Acknowledgments

The author B. Rossi acknowledges the financial support of the Regione Veneto, being the beneficiary of a scholarship within the Programma Operativo Regionale FSE 2007-2013.

References

[1] J. Szejtli, *Chem. Rev.* **1998**, *98*, 1743.
[2] M. L. Bender, M. Komiyama, *Cyclodextrin chemistry*, Springer-Varlag, New York, **1978**.
[3] J. Szejtli, *Cyclodextrin technology*, Kluwer Academic Publishers, Boston, **1988**.
[4] V. Crupi, G. Guella, D. Majolino, I. Mancini, A. Paciaroni, B. Rossi, V. Venuti, P. Verrocchio, G. Viliani, *Phil. Mag.* **2011**, *91*, 1776.
[5] V. Crupi, G. Guella, D. Majolino, I. Mancini, B. Rossi, R. Stancanelli, V. Venuti, P. Verrocchio, G. Viliani, *Food Biophysics* **2011**, *6*, 267.
[6] C. Cannavà, V. Crupi, M. Guardo, D. Majolino, R. Stancanelli, S. Tommasini, C. A. Ventura, V. Venuti, *J. Incl. Phenom. Macrocycl. Chem.* **2012**, DOI: 10.1007/s10847-012-0110-3.
[7] D. Duchene, *New Trends in Cyclodextrins and Derivatives*, Editions de Santè, Paris, **1991**.
[8] F. Trotta, W. Tumiatti, Patent WO 03/085002, **2003**.
[9] F. Trotta, W. Tumiatti, R. Cavalli, O. Zerbinati, C. M. Roggero, R. Vallero, Patent number WO 06/002814, **2006**
[10] F. Trotta, R. Cavalli, *Compos. Interface.* **2009**, *16*, 39.
[11] F. Castiglione, V. Crupi, D. Majolino, A. Mele, W. Panzeri, B. Rossi, F. Trotta, V. Venuti, *J. Incl. Phenom. Macrocycl. Chem.* **2012**, DOI: 10.1007/s10847-012-0106-z.
[12] L. Seglie, K. Martina, M. Devecchi, C. Roggero, F. Trotta, V. Scariot, *Plant Growth Regul.* **2011**, *65*(3), 505.
[13] B. B. Mamba, R. W. Krause, T. J. Malefetse, G. Gericke, S. P. Sithole, *Water SA* **2008**, *34*, 657.
[14] M. Arkas, R. Allabashi, D. Tsiourvas, E. M. Mattausch, R. Perfler, *Environ. Sci. Technol.* **2006**, *40*, 2771.
[15] J. Alongi, M. Poskovic, P. M. Visakh, A. Frache, G. Malucelli, *Carbohyd. Polym.* **2012**, *88*(4), 1387.
[16] D. Enescu, J. Alongi, A. Frache, *J. Appl. Polym. Sci.* **2012**, *123*(6), 3545.
[17] P. K. Shende, F. Trotta, R. S. Gaud, K. Deshmukh, R. Cavalli, M. Biasizzo, *J. Incl. Phenom. Macrocycl. Chem.* **2012**; *74*(1-4), 447.
[18] F. Trotta, R. Cavalli, K. Martina, M. Biasizzo, J. Vitillo, S. Bordiga, P. Vavia, J. Ansari, J. Incl. Phenom. *Macrocycl. Chem.* **2011**, *71*(1-2), 189.
[19] F. Trotta, W. Tumiatti, R. Cavalli, C. M. Roggero, B. Mognetti, G. Berta Nicolao, Patent WO 09/003656, **2009**.
[20] A. Vyas, S. Shailendra, S. Swarnlata, *J. Incl. Phenom. Macrocycl. Chem.* **2008**, *62*, 23.
[21] S. Swaminathan, P. R. Vavia, F. Trotta, S. Torne, *J. Incl. Phen. Macroc. Chem.* **2007**, *57*, 89.
[22] B. Boscolo, F. Trotta, E. Ghibaudi, *J. Mol. Catal. B: Enzym.* **2010**, *62*, 155.
[23] S. Swaminathan, L. Pastero, L. Serpe, F. Trotta, P. Vavia, D. Aquilano, M. Trotta, G. Zara, R. Cavalli, *Eur. J. Pharm. Biopharm.* **2010**, *74*, 193.
[24] K. Ansari, P. Vavia, F. Trotta, R. Cavalli, *AAPS Pharm. Sci. Tech.* **2011**, *12*(1), 279.
[25] R. Cavalli, A. Akhter, A. Bisazza, P. Giustetto, F. Trotta, P. Vavia, *Int. J. Pharm.* **2010**, *402*(1-2), 254.
[26] F. Castiglione, V. Crupi, D. Majolino, A. Mele, B. Rossi, F. Trotta, V. Venuti, *J. Phys. Chem. B* **2012**, *116*(43), 13133.

[27] B. Rossi, S. Caponi, F. Castiglione, S. Corezzi, A. Fontana, M. Giarola, G. Mariotto, A. Mele, C. Petrillo, F. Trotta, G. Viliani, *J. Phys. Chem. B* **2012**, *116* (17), 5323
[28] A. Mele, F. Castiglione, L. Malpezzi, F. Ganazzoli, G. Raffaini, F. Trotta, B. Rossi, A. Fontana, G. Giunchi, J. Inclusion *Phenom. Macrocyclic Chem.* **2011**, *69*, 403.
[29] F. Castiglione, V. Crupi, D. Majolino, A. Mele, B. Rossi, F. Trotta, V. Venuti, *J. Phys. Chem. B* **2012**, *116*(27), 7952.
[30] V. Crupi, F. Longo, D. Majolino, V. Venuti, *J. Phys.: Condens. Matt.* **2006**, *18*, 3563.
[31] D. Hadzi, S. Bratos, *The Hydrogen Bond*, (Eds.: P. Schuster, G. Zundel, C. Sandorfy), North-Holland Publishing and Co., Amsterdam, North-Holland, Amsterdam, **1976**.
[32] P. A. Kollman, L. C. Allen, *Chem. Rev.* **1972**, *72*, 283.
[33] N. A. Chumaevskii, M. N. Rodnikova, *J. Mol. Liq.* **2003**, *106*, 167.
[34] F. N. Keutsch, R. J. Saykally, *Proc. Natl. Acad. Sci. U. S. A.* **2001**, *98*, 10533.
[35] J. D. Eaves, J. J. Loparo, J. C. Fecko, S. T. Roberts, A. Tokmakoff, P. L. Geissler, *Proc. Natl. Acad. Sci. U. S. A.* **2005**, *2*, 13019.
[36] D. P. Schofield, J. R. Lane, H. G. Kjaergaard, *J. Phys. Chem. A* **2007**, *111*, 567.
[37] N. Goldman, R. J. Saykally, *J. Chem. Phys.* **2004**, *120*, 4777.
[38] F. Mallamace, M. Broccio, C. Corsaro, A. Faraone, D. Majolino, V. Venuti, L. Liu, C. Y. Mou, S. H. Chen, *Proc. Natl. Acad. Sci. U. S. A.* **2007**, *104*, 424.
[39] M. Freda, A. Piluso, A. Santucci, P. Sassi, *Appl. Spectrosc.* **2005**, *59*, 1155.
[40] D. A. Schmidt, K. Miki, *J. Phys. Chem. A* **2007**, *111*, 10119.
[41] K. Ohno, M. Okimura, N. Akai, Y. Katsumoto, *Phys. Chem. Chem. Phys.* **2005**, *7*, 3055.
[42] J. B. Brubach, A. Mermet, A. Filabozzi, A. Gerschel, D. Lairez, M. P. Krafft, *J. Phys. Chem. B* **2001**, *105*, 430.
[43] C. Corsaro, V. Crupi, D. Majolino, V. Venuti, U. Wanderlingh, *J. Phys. Chem. B* **2008**, *112*, 3927, and references therein.
[44] F. Mallamace, S. H. Chen, M. Broccio, C. Corsaro, V. Crupi, D. Majolino, V. Venuti, P. Baglioni, E. Fratini, C. Vannucci, H. E. Stanley, *J. Chem. Phys.* **2008**, *127*, 045104, and references therein.
[45] V. Crupi, D. Majolino, P. Migliardo, V. Venuti, M. C. Bellissent-Funel, *Mol. Phys.* **2003**, *101*, 3323.
[46] R. Bergman, J. Swanson, *Nature* **2000**, *403*, 283.
[47] V. Crupi, F. Longo, D. Majolino, V. Venuti, *J. Chem. Phys.* **2005**, *123*, 154702.
[48] R. Stancanelli, R. Ficarra, C. Cannavà, M. Guardo, M. L. Calabrò, P. Ficarra, R. Ottanà, R. Maccari, V. Crupi, D. Majolino, V. Venuti, *J. Pharm. Biomed. Anal.* **2008**, *47*, 704.
[49] K. B. Møller, R. Rey, J. T. Hynes, *J. Phys. Chem. A* **2004**, *108*, 1275.
[50] C. P. Lawrence, J. L. Skinner, *Chem. Phys. Lett.* **2003**, *369*, 472.
[51] I. Bratu, F. Veiga, C. Fernandes, A. Hernanz, J. M. Gavira, *Spectroscopy* **2004**, *18*, 459.
[52] T. Corridoni, A. Sodo, F. Bruni, M. A. Ricci, M. Nardone, *Chem. Phys.* **2007**, *336*, 183.
[53] V. Crupi, S. Interdonato, F. Longo, D. Majolino, P. Migliardo, V. Venuti, *J. Raman Spectrosc.* **2008**, *39*, 244.
[54] P. A. Giguère, *J. Chem. Phys.* **1987**, *87*, 4835.